

# Dynamic Demagnetization Model of Permanent Magnets for Finite Element Analysis

P. Zhou<sup>1</sup>, D. Lin<sup>1</sup>, Y. Xiao<sup>1</sup>, N. Lambert<sup>1</sup> and M.A. Rahman<sup>2</sup>

<sup>1</sup>Ansys Inc, 225 W. Station Square Dr., Pittsburgh 15219 USA Ping.zhou@ansys.com

<sup>2</sup>Memorial University of Newfoundland, St. John's, NL, A1B 3X5 Canada arahman@mun.ca

**Abstract** — this paper presents a linearized demagnetization model taking into account temperature dependence. At the same time, an efficient searching algorithm is proposed to properly identify the new worst working point and update the recoil line during the entire transient solution process if a working point is discovered below the knee point of the current recoil line. This model is extended to take into account the temperature dependence of demagnetization behaviors.

## I. INTRODUCTION

Recently, different demagnetization modeling techniques based on finite element analysis (FEA) have been discussed in the literature. Kang *et al.* presented a two-step approach to first determine the worst load condition from transient solutions, and then apply this worst load condition to the irreversible demagnetization analysis using 2D magneto-static FEA[1]. The demagnetization has also been modeled by the classical Preisach-type hysteresis model to analyze the demagnetization states of permanent magnets during fault conditions in large synchronous motors [2]. Ruoto *et al.* have introduced an exponential function based model to take into account the temperature dependence of demagnetization behavior [3]. Clearly, the two-step approach ignored the demagnetization impact on transient solutions, thus the discovered worst working point may not represent the true operating condition. Therefore, it is necessary to check the working point of each element at each time-step. If the working point is too far from the curve given by the demagnetization model, the remanence of that element has to be adjusted so that the working point is brought back to the BH curve [3]. On the other hand, how a new worst load point is identified will have a direct impact on modeling accuracy, computation efficiency and convergence.

This paper introduces a linear model that handles the complete demagnetization curve and temperature dependence of demagnetization behaviors. At the same time, an efficient searching algorithm is proposed to iteratively search for a new worst working point along the gradient direction from time to time during the entire transient solution process if a working point is discovered below the knee point of the current recoil line. Then, this model is further extended to take into account the temperature dependent demagnetization behaviors.

## II. IRREVERSIBLE DEMAGNETIZATION MODEL

If the working point  $a$  of permanent magnet material goes below the knee point  $K$  by an external field  $H_a$ , even after the external field  $H_a$  is reduced or totally removed, the subsequent working point will no longer along the original B-H curve, but along the recoil line  $L_a$ . As long as the subsequent applied external demagnetization field intensity does not exceed  $H_a$ , the permanent magnet will work along the recoil line  $L_a$ . If, however, greater external demagnetization field  $H_b$  is applied,

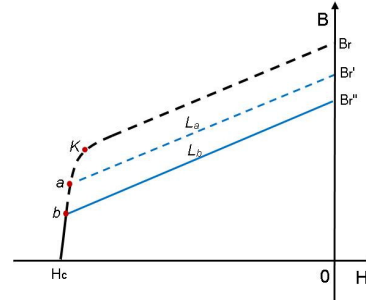


Fig. 1 Irreversible demagnetization due to working point below the knee point a lower knee point  $b$  associated with a new recoil line  $L_b$  will be established as indicated in Fig. 1.

During FE analysis, the permanent magnet represented by the coercivity  $H_c$  is treated as an additional source contributing to the right-side hand of the FE formulation. The proposed approach is based on a linearized model characterized by the recoil line passing through the latest identified demagnetization point. This point will be updated from time to time when a new worst working point is discovered. In the model, the value of coercivity used in the FE formulation is  $H_c'$ , the intersection of the recoil line with H-axis, as shown in Fig. 2, not  $H_c$ , directly from the original demagnetization curve. At the same time, the linear permeability with the value of the slope of the recoil line is used. Clearly, this linear model is valid only when the working point is above the worst point  $K$  on the recoil line such as the point  $P_1$ . This suggests that it is necessary to check the validity of the working point on the recoil line for every element at each time step. If a working point is discovered below the point  $K$  on the recoil line as the point  $P_2$ , a new and lower point  $K'$  corresponding to a new worst working point has to be identified from the original demagnetization curve during the transient process. The key issue here is how to efficiently identify this new worst working point  $K'$  from the original demagnetization curve. This will be described in detail as follows.

Assume that the point  $K_0$  in Fig. 3 is the worst working point so far during the transient FE analysis, and the working point  $P_1$  is derived based on  $H_{c0}$  associated with the recoil line  $L_0$  passing through the point  $K_0$ . Since the working point  $P_1$  is

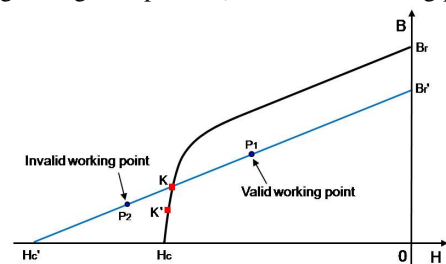


Fig. 2 Linearized demagnetization model

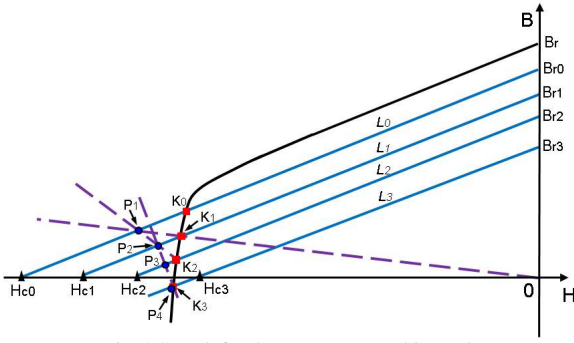


Fig. 3 Search for the new worst working point

below the point  $K_0$ , this linear model is no longer valid and a new and lower worst working point has to be identified. Clearly, this new worst working point should also reside on the original demagnetization curve. To this end, let us first to draw a line linking the origin with the working point  $P_1$ . The intersection between this line and the original demagnetization curve, the point  $K_1$ , is the candidate of the new worst working point to be searched for. It follows that after the FE analysis at the same time instant based on  $H_{ci}$  associated with the recoil line  $L_1$ , a new working point  $P_2$  can be derived. Since the working point  $P_2$  does still not reside on the original demagnetization curve, the searching process has to continue.

We could repeat the above scheme by drawing a line linking the origin with the working point  $P_2$  to obtain a new candidate of the worst working point. But the convergence is very slow. Instead, searching in the gradient direction along the line passing through both the previous working point  $P_1$  and the current working point  $P_2$  is much more efficient. The intersection between this line and the original demagnetization curve,  $K_2$ , provides an improved candidate for the new worst working point. Consequently, a new working point  $P_3$  can be derived after FE analysis based on the updated recoil line  $L_2$  with  $H_{c2}$ . Even though  $P_3$  has not moved onto the original demagnetization curve yet, the new point  $P_3$  is much closer compared to the previous point  $P_2$ .

Similarly, by searching in the gradient direction along a line passing through both the previous working point  $P_2$  and the current working point  $P_3$ , the intersection between this line and the original demagnetization curve,  $K_3$ , provides a new linear model characterized by the recoil line  $L_3$  with  $H_{c3}$ . The subsequent FEA simulation will provide a new working point  $P_4$ . As the working point  $P_4$  has converged onto the original demagnetization curve within a pre-specified tolerance,  $K_3$  is the new worst working point. Since the searching algorithm converges along the gradient direction, only a very few iterations are required to find the new worst working point.

### III. TEMPERATURE DEPENDENT DEMAGNETIZATION MODEL

For a better representation of any type of magnet, it is advantageous to work on intrinsic flux density  $B_i$  vs  $H$  curve, instead of flux density  $B$  vs  $H$  curve. Once the temperature dependent  $B_i$ - $H$  curve is derived, it is straightforward to convert  $B_i$ - $H$  characteristic into  $B$ - $H$  characteristic in terms of

$$B = B_i + \mu_0 H \quad (1)$$

In the model, two temperature dependent parameters are remanent flux density  $B_r$ , the value of  $B_i$  (or  $B$ ) at  $H = 0$ , and

intrinsic coercivity  $H_{ci}$ , the value of  $H$  at  $B = 0$ . Both  $B_r$  and  $H_{ci}$  can be described using second order polynomials as

$$B_r(T) = B_r(T_0)(1 + \alpha_1(T - T_0) + \alpha_2(T - T_0)^2) = B_r(T_0)P(T) \quad (2)$$

$$H_{ci}(T) = H_{ci}(T_0)(1 + \beta_1(T - T_0) + \beta_2(T - T_0)^2) = H_{ci}(T_0)Q(T) \quad (3)$$

where  $T_0$  is the reference temperature, and  $\alpha_1$ ,  $\alpha_2$ ,  $\beta_1$  and  $\beta_2$  are coefficients which can be identified from supplier datasheets.

The  $B_i$ - $H$  curve up to the intrinsic coercivity  $H_{ci}$  can be described by the following function:

$$B_i(H, T) = P(T) \left( b_0 \tanh\left(\frac{H + Q(T)H_{ci}(T_0)}{Q(T)h_0}\right) + b_1 \tanh\left(\frac{H + Q(T)H_{ci}(T_0)}{Q(T)h_1}\right) \right) \quad (4)$$

Here  $P(T)$  and  $Q(T)$  are defined by (2) and (3), respectively. They are both unit at the reference temperature  $T_0$ . As a result, all coefficients  $b_0$ ,  $h_0$ ,  $b_1$  and  $h_1$  can be identified by a nonlinear curve fitting based on  $B_i$ - $H$  curve at the reference temperature  $T_0$ . It can be easily verified that (4) has automatically satisfied the constraint of (2):  $B_i(0, T) = B_r(T)$ . Consequently, once the model is constructed at the reference temperature  $T_0$ , any  $B_i$ - $H$  curves at other temperature can be dynamically reconstructed in terms of the temperature dependence of  $B_r(T)$  and  $H_{ci}(T)$ . Finally, the  $B$ - $H$  curve in the second and third quadrants can be further derived through (1), and the temperature dependent slope of the recoil line is derived from (1) and (4) as

$$\mu(T) = \left. \frac{\partial B(H, T)}{\partial H} \right|_{H=0} = \left. \frac{\partial B_i(H, T)}{\partial H} \right|_{H=0} + \mu_0 = \frac{P(T)}{Q(T)} \mu_i(T_0) + \mu_0 \quad (5)$$

### IV. BENCHMARK EXAMPLE

The proposed model is applied to 3D FE analysis of a 8-pole, 48-slot Toyota Prius IPM motor [4]. Fig. 4 shows the torque derived without considering demagnetization of NdFeB magnets, and with considering demagnetization of NdFeB magnets at temperatures of 25° and 90°, respectively. More results will be provided in the full paper.

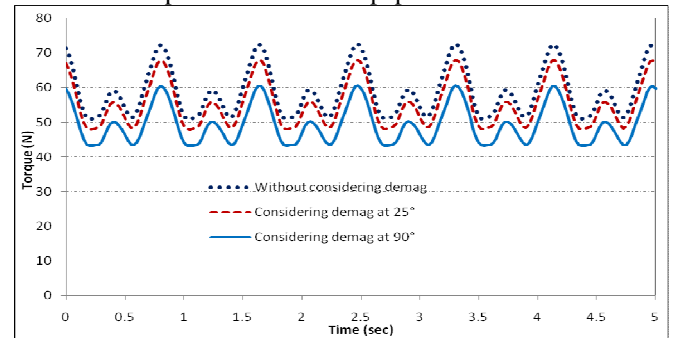


Fig. 4. Torque profiles showing temperature dependent demagnetization effects

### V. REFERENCES

- [1] G.H. Kang, *et al.*, "Analysis of irreversible magnet demagnetization in line-start motors based on the finite-element method", *IEEE Trans. on Magnetics*, vol. 39, no. 3, pp. 1488-1491, May, 2003.
- [2] M. Rosu, *et al.*, "Hysteresis model for FE analysis of permanent-magnet demagnetization in a large synchronous motor under a fault", *IEEE Trans. on Magnetics*, vol. 41, no. 6, pp. 2118-2123, June, 2005.
- [3] S. Ruoho, *et al.*, "Interdependence of demagnetization, loading and temperature rise in a permanent-magnet synchronous motor", *IEEE Trans. on Magnetics*, vol. 46, no. 3, pp. 949-953, March, 2010.
- [4] J.S. Hsu, *et al.*, "Report on Toyota/Prius Motor Torque Capability, Torque Property, No-Load Back EMF, and Mechanical Losses", Oak Ridge National Laboratory, Oak Ridge Institute for Science and Education, ORNL/TM-2004/185.